Proceedings World Geothermal Congress 2020+1
Reykjavik, Iceland, April - October 2021

Reservoir Tracer Testing at San Jacinto-Tizate Geothermal Production Field, Nicaragua

Julio Alberto Guidos Pineda[1], Lester Lenin Prado[1], Idalia Matus[1],
Gregory N. Ussher[2] and Ramonchito Cedric M. Malate[2]

[1]Polaris Energy Nicaragua S.A. (PENSA), Km 114 Carretera Leon-Malpaisillo, San Jacinto, Leon, Nicaragua
[2]Jacobs New Zealand, Level 2, Carlaw Park, 12-16 Nicholls Lane, Parnell, Auckland, New Zealand

jguidos@polaris.com, ramonchito.malate@jacobs.com

Keywords: San Jacinto geothermal field, reservoir tracer test, reservoir monitoring

ABSTRACT

The San Jacinto-Tizate Geothermal Production Field in Nicaragua was developed by Polaris Energy Nicaragua S.A. (PENSA) for power production since 2005. A 10 MWe back pressure power plant was initially installed in the field and was decommissioned in 2012 after the full planned development of 72 MWe condensing plant (2 x 36 MWe units) began operation. PENSA implemented reservoir management strategies for the sustainability of the resource through intensive monitoring, one of which is reservoir tracer testing.

A series of reservoir tracer tests using naphthalene disulfonate salts (NDS) was conducted by PENSA with the main objective of quantifying the rate and extent of brine injection returns from the northern, infield and southern injection wells to the central production wells. The tracer tests were conducted after commissioning of the condensing plants in 2011 and completing the production drilling and well remedial operations in January 2014. The reservoir tracer test in 2015 was conducted to validate/confirm the positive tracer returns from the southern injection well SJ10-1 based on earlier tests conducted in July 2012 and also to determine the effects of prolonged infield injection at SJ12-1 ST1 which was not evaluated in the earlier tracer test.

Positive tracer returns were observed in production wells SJ4-1, SJ6-2 and SJ9-1 from the injection fluids coming from SJ10-1. The tracer return curves were processed and interpreted using simple radial flow tracer model. Modelling of NDS tracer recoveries in the affected wells gave a fraction of returning fluid ranging from 10% to 16%. The return of injection fluids into SJ4-1 has resulted in gradual decline in measured temperature in the well. This thermal decline is modelled by coupling the chloride mass balance model to a fracture flow model. The simple heat advection model satisfactorily represented the thermal decline observed in the well.

The reservoir tracer tests implemented in San Jacinto geothermal production field helped understand the hydrological connection of northern and southern injection wells to the main production area together with the impact of limited infield injection. The results of reservoir tracer testing have also provided PENSA the flexibility to optimize injection and balance pressure support against the risk of reservoir cooling.

1. INTRODUCTION

The San Jacinto-Tizate geothermal field is located in northwestern Nicaragua, approximately 20 km northeast of the city of Leon that is centrally situated among a series of active volcanoes (Figure 1). The initial phase of exploration drilling conducted in 1993-1995 by Russian company Intergeotherm S.A. confirmed a liquid-dominated reservoir with temperatures of 260°C – 300°C in the central upflow area and benign chemistry. The field was acquired in 2003 by Polaris Energy Nicaragua S.A. (PENSA) who engaged Jacobs (formerly Sinclair Knight Merz, SKM) to evaluate the resource potential and develop and implement a strategy for the commercial development of the resource.

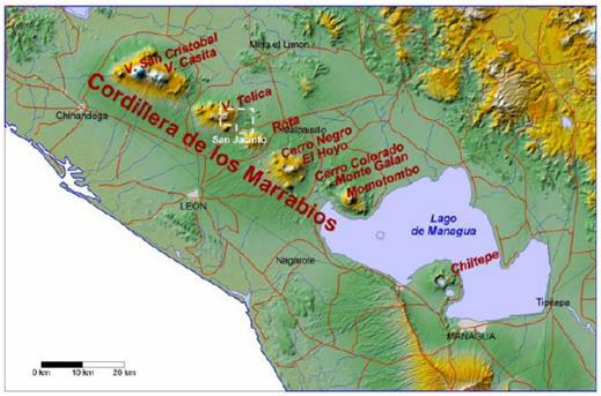

Figure 1: San Jacinto=Tizate geothermal project location.

Geochemical changes in the production wells in addition to production temperature and enthalpy are monitored throughout the period of exploitation of the San Jacinto reservoir. By recording changes in these parameters, field management strategies are developed and implemented. The most commonly measured geochemical parameters are the chloride and silica content of the produced fluid.

The deeper-producing, hotter wells at San Jacinto (SJ5-1, SJ6-2, SJ9-3 and SJ12-2) have shown little change in discharge chemistry since commissioning of the plants. There is no evidence for cooling due to ingress of peripheral ground waters. However, the shallow–producing well SJ4-1 has shown geochemical changes, in particular, an increase in reservoir chloride and a decline in CO_2 gas concentrations almost immediately after cut-in of the well as shown in Figure 2 and Figure 3 (Jacobs 2015a).

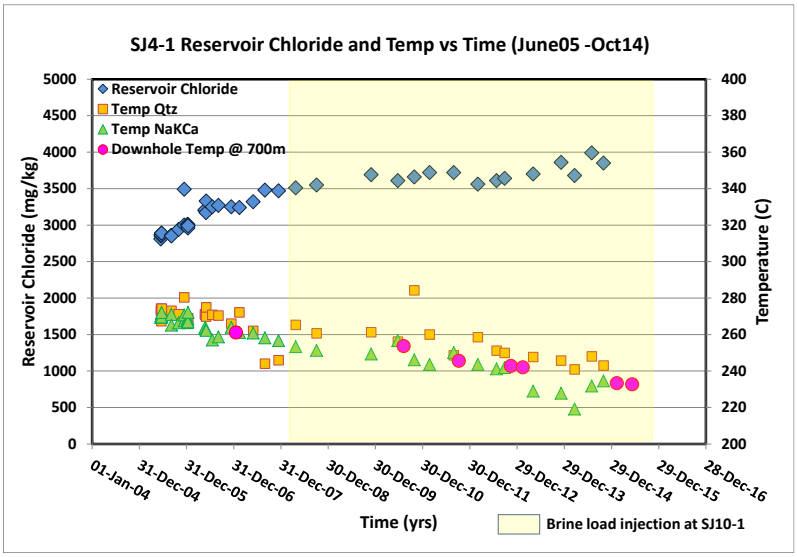

Figure 2: SJ4-1 production chloride and temperature with time (2005-2014).

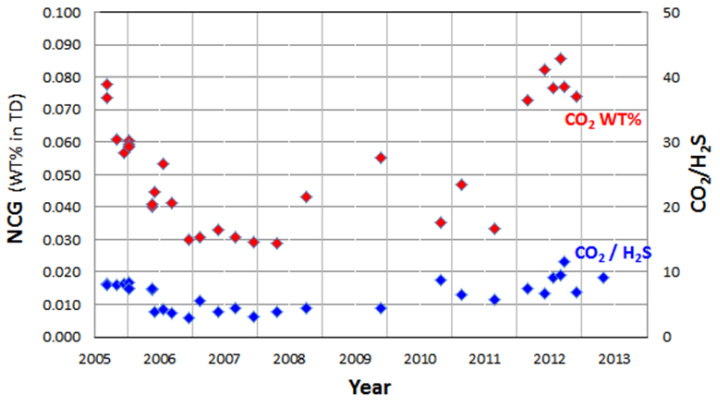

Figure 3: SJ4-1 CO_2 discharge chemistry with time (2006-2013).

The reservoir chloride concentration increased during the first year of production and then stabilized at about 3,300 ppm with the gas content falling from 0.08 to 0.04 wt%. Quartz temperatures remained essentially constant during the first year but slower equilibrating cation geothermometers (T_{NaKCa}) declined slowly.

The trend to 2008 suggests recharge by cooler, degassed brine, naturally occurring within the shallow reservoir. It is unlikely that injection returns were responsible for this early rapid change because injection during this time was deep and some distance away from SJ4-1. The reservoir chloride between April and October 2008 increased again, coincident with the start of injection to SJ10-1. The injection zone in SJ10-1 is probably in the same aquifer as that produced by SJ4-1 so injection returns of high chloride brine is possible. The reservoir chloride increase during that period would require movement of injection fluids across 1.6 km in at least 6 months (>>8 m per day).

There appears to be partial levelling out of chloride trend, with total discharge gas content increasing in 2009. The reason for this could be due to partial reduction in injection load from SJ10-1 following commissioning of the new SJ11-1 injection well in the northern part of the field. Continued increase in reservoir chloride was observed when full operation of the power plants started in 2011 with all injection wells on line.

The gas content reached its lowest point (~0.03 wt%) in 2008 but has since increased to around 0.08 wt%, close to the commissioning concentration of about 0.1 wt%. This is at odds with the chloride and temperature data which indicates recharge by boiled, degassed brine. The higher gas content is probably partly due to a small amount of excess enthalpy at the field zone. The enthalpy data is sparse for this period but there are a few measurements showing about 100 kJ/kg in excess enthalpy.

A decline in feed-zone temperature since 2005 can also be seen in SJ4-1, by about 10°C based on T_{QTZ} and enthalpy measurements as shown in Figure 2. Calculated TFT enthalpy results (1,090-1,150 kJ/kg) indicate feed-zone temperatures of 250-260°C, lower than original temperatures of about 265°C. T_{NaKCa} geothermometer temperatures, reflecting temperatures closer to the source of recharge, have declined by at least 20°C, from 265 to 245°C. Downhole static temperature measurements taken in the well at 700 meters near the main permeable zone also showed cooling by about 30°C since 2005.

The well's enthalpy has declined at the start of production but remained constant throughout its utilization until a small decline in enthalpy was later observed. There are probably competing processes of (1) pressure drawdown stimulating boiling and (2) cooler water recharge suppressing boiling.

A series of reservoir tracer tests using naphthalene disulfonate salts (NDS) were then conducted by PENSA with the following objectives: 1) quantify the rate and extent of brine injection returns from the northern, infield and southern injection wells to the central production wells, 2) identify fluid flow paths/channels of the returning brine and 3) to predict possible cooling rates of production wells due to injection returns. The tracer tests were conducted after commissioning of the 2x36 MWe condensing plants in 2011 and completing the production drilling and well remedial operations in January 2014 to improve and sustain the steam availability at San Jacinto. The reservoir tracer test in 2015 was conducted to validate/confirm the positive tracer returns from the southern injection well SJ10-1 based on earlier tests conducted in July 2012 and also to determine the effects of prolonged infield injection at SJ12-1 ST1 which was not evaluated in the earlier tracer test.

A lumped parameter model of production chloride has been developed to model the effects of injection returns to the production sector. The chloride mass balance model developed aims to match the chloride increase at SJ4-1. For the system considered here, the reservoir fluid is extracted from the production sector and the hot water is passed through a separator where steam is separated and fed to the turbine to produce power. For the purpose of maintaining reservoir pressure and environmental concerns, the reject water is returned into the system. A high permeability fracture zone is assumed to connect the production and injection sectors.

The fast return of the injection fluids is often attributed to preferential pathways (fracture zone) from the production to the injection sector. The most serious problem associated with an increase in the rate of injection fluid returning to the production sector is decline in the production temperature.

The temperature decline in SJ4-1 is then modelled by coupling the chloride mass balance model to a one dimensional fracture flow model. Various models can be considered for the fracture zone connecting the injection and production wells. The simplest model presented here assumes the heat is transported primarily by advection along the fractured zone and that diffusion of heat from the fractured zone to the less permeable surrounding rock is assumed to be small. Hence the energy carried by the injection fluid is conserved due to the fluid's bulk motion.

2. RESERVOIR TRACER TESTS

The reservoir tracer tests in 2012 and 2015 were conducted by PENSA and the tracer sample analysis by LaGeo. The chemical tracers were introduced to four injection wells in 2012 and another injection well (SJ12-1 ST1) included in the tracer test in 2015. Five naphthalene sulfonic acid tracers with different chemical structures were introduced in 2015 into the five injection wells SJ1-1, SJ9-2 ST3, SJ10-1, SJ11-1 and SJ12-1 ST1 so that the source of any injection return could be linked to its injection source. Tracer quantities injected in 2015 are given in **Error! Not a valid bookmark self-reference.** below. Baseline tracer samples are also collected before the tracer injection.

Each tracer injection was readied by preparing 1.0 m^3 of fresh water in a tank in which the chosen salt was slowly dissolved prior to injection. A mechanical stirrer provided agitation to the salt solution during the process. After the tracer was injected into the injection well, pumping of fresh water was continued until approximately 2.0 m^3 had been pumped into the well to ensure cleanliness of the pumping equipment and positive displacement of the chemical tracer into the injection well. Daily tracer samples collected were analyzed to monitor for tracer concentrations from production wells SJ4-1, SJ5-1, SJ6-1, SJ6-2, SJ9-1, SJ9-3, SJ12-2 and SJ12-3; commencing on the day of the first tracer injection test.

Table 1: Reservoir Tracer Quantities Injected (2015).

Injection Well	Chemical Tracer Injected	Quantity Injected
SJ9-2 ST3	1,5 naphthalene di-sulfonic acid	150 kg
SJ10-1	1,3,5 naphthalene tri-sulfonic acid	150 kg
SJ11-1	1-6 naphthalene di-sulfonic acid	150 kg
SJ12-1 ST1	2 naphthalene-sulfonic acid	150 kg
SJ1-1	1 naphthalene sulfonic acid	150 kg

2.1 SJ10-1 Tracer Injection Results (2015)

After 106 days of tracer monitoring, only two chemical tracers had been detected in the production wells, i.e.: the 1,3,5 naphthalene tri-sulfonic acid (1,3,5 NTS) introduced into SJ10-1 and 2 naphthalene sulfonic acid (2 NS) injected into SJ12-1 ST1. The 1,3,5 NTS tracer was only detected in SJ4-1, SJ6-2 and SJ9-1, as shown by the tracer concentration plot in Figure 4. No trace of the 1,3,5 NTS were detected in SJ5-1, SJ6-1, SJ9-3, SJ12-2 and SJ12-3.

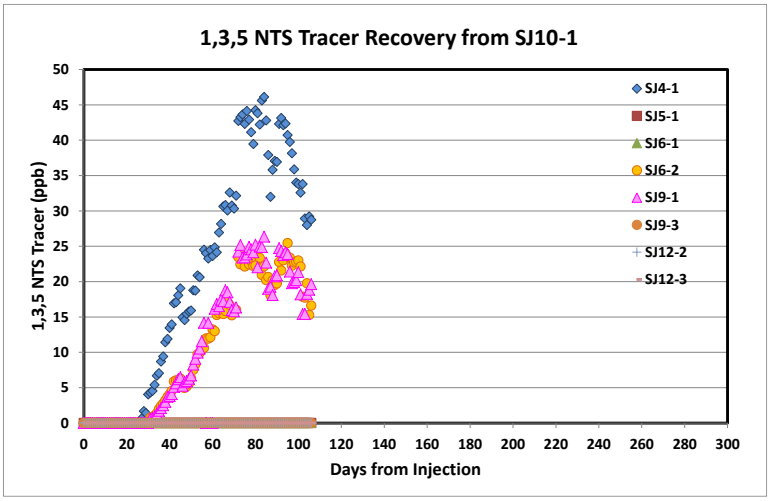

Figure 4: Plot of 1,3,5 NTS tracer concentrations in SJ production wells (from LaGeo 2015).

Arrival of the 1,3,5 NTS tracer in SJ4-1 was detected 28 days after its injection at SJ10-1 followed by tracer arrival of 33 days in SJ6-2 and 34 days in SJ9-1. These tracer arrival times are similar to the tracer breakthrough times observed during the previous reservoir tracer test in 2012.

2.2 Tracer Recovery Modelling

The tracer recovery in the affected production wells was about 50% with about three months of tracer sampling. This provided initial confidence in attempting to model the tracer recoveries over the full extrapolated return period. Jacobs modelled the amounts of tracer recovered using a radial flow model and the tracer modelling software Anduril 2.3 (2005). The remaining tracer concentration returns were modelled assuming a typical exponential decay function for the least squares approximation fitting calculation of the complete tracer recovery profile. The tracer concentration profile calculated for SJ4-1 is presented in Figure 5 below.

The standard radial flow tracer model can be defined by the following relationship with the tracer concentration given by:

$$C(t) = \left\{\frac{A_0}{\pi h \phi S_w x^2}\right\}\left\{\frac{F}{\sqrt{4\pi\frac{D_1}{vx}t^3}}\right\} e^{-\frac{(1-t)^2}{4\frac{D_1}{vx}t}} \qquad (1)$$

where $C(t)$ = tracer concentration; x = interwell distance; t = normalized time; S_w – water saturation; A_0 = injected tracer activity; D_1/vx = dispersivity; h = layer thickness; F = scale factor; ϕ = porosity

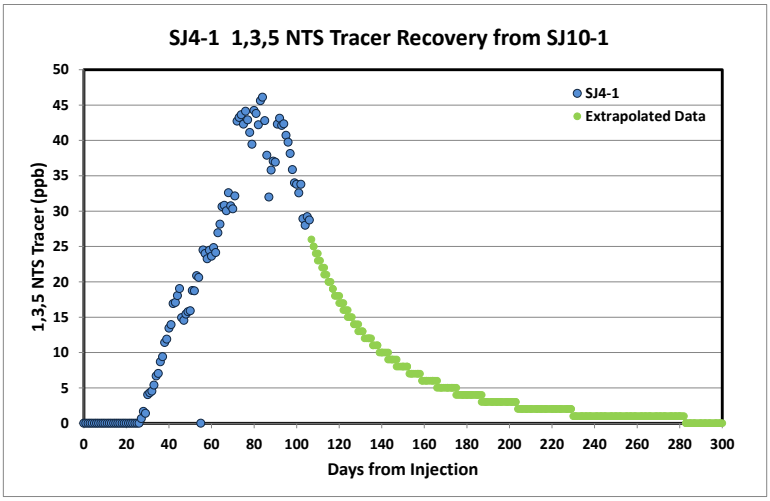

Figure 5: SJ4-1 tracer concentration profile with extrapolated data using exponential decay function.

Here, the linear distance between SJ4-1 and SJ10-1 is given at around 1,620 meters, the reservoir porosity is conservatively assumed at 5.0% and a layer thickness of 100 meters. The model fitting parameters dispersivity (D_1/vx), scale factor (F) and mean transit time were then varied to match the measured tracer concentration profile. The match to the measured tracer recovery data for SJ4-1 is presented in Figure 6 below. The model parameters and model results are summarized in **Table 2**. The results show that about 16% of the water injected into SJ10-1 is eventually produced by SJ4-1. The tracer returns identify a permeable shallow

route for potential recharge that may be drawing in other cooler waters (e.g. existing groundwater and shallow brine), as well. It is noted that SJ4-1 displayed some degree of cooling even before SJ10-1 was used for hot brine injection.

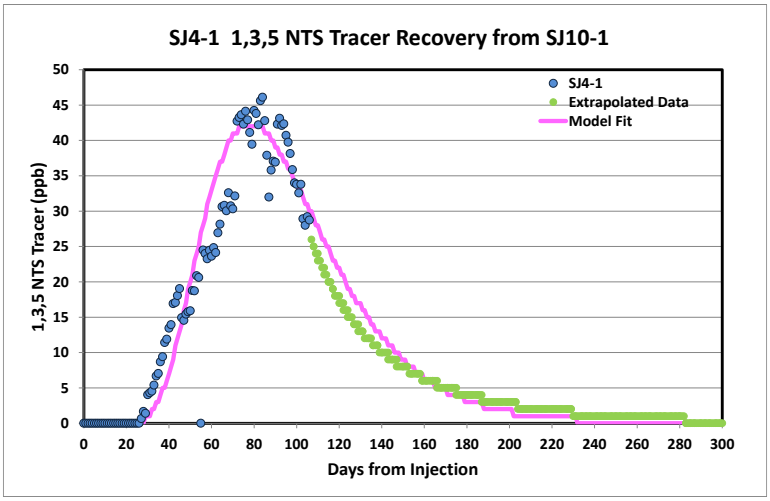

Figure 6: SJ4-1 tracer concentration profile with model results.

The average velocity of tracer between injection well SJ10-1 and SJ4-1 can be estimated from the horizontal distance and time of first tracer arrival (breakthrough time). The calculated tracer velocity from injection well SJ10-1 is about 2.45 m/hr which is in the range measured at other geothermal fields around the world with similar geological characteristics. For example, in several tracer injection tests at Wairakei in the early 1980's, tracer velocities of 1 to 5 m/hr were measured and were described as 'moderate' compared to other fractured fields around the world (Fossum and Horne, 1982). For comparison, in one case at Wairakei a velocity of ~100 m/hr was measured, indicating rapid, short-circuited flow along faults. Reservoir tracer injection tests have been conducted and returns observed at many geothermal fields around the world, including Southern Negros, Tongonan, Mt Apo, Los Azufres, Wairakei, Ohaaki, Gunung Salak and Dixie Valley.

Table 2: Results of 1,3,5 NTS tracer recovery for SJ4-1.

Parameters	SJ4-1
Amount of 1,3,5 NTS tracer injected (kg)	150
Linear distance from SJ10-1 (m)	~1,620
Layer thickness (m)	100
Porosity (%)	5.0
Dispersivity D_1/vx	0.065
Scale factor F	9.0
Breakthrough Time (days)	28
Mean transit time (days)	99
Well total mass flow rate (t/hr)	370
Steam Mass Fraction	0.234
Brine flow rate (t/hr)	283
1,3,5 NTS tracer recovered (kg)	23.49
Percentage recovered (%)	15.7%

3. LUMPED PARAMETER MODEL OF CHLORIDE CONCENTRATION INCREASE

A lumped parameter model of chloride concentration increase described by Malate and O'Sullivan (1990) was employed in this modeling study. The simple production and injection model is illustrated in Figure 7. This consists of a production sector, injection sector and a recharge sector. The basic assumptions used in the model are:

1) There is no change in the mass of fluid stored in each of the production and injection sectors.
2) The chloride concentration $[Cl]_{rec}$ of the recharge flow REC is constant during the period of exploitation.
3) The production enthalpy remains constant.
4) The fraction of injection fluid returning to the production area is constant.
5) The time delay of the chloride concentration returning $[Cl]_{ret}$ is assumed to be small.

These assumptions are considered valid for short term reservoir behavior while the thermodynamic state of the reservoir is changing slowly. The third assumption allows the model equations for the chloride concentration, silica concentration and temperature to be decoupled.

A chloride mass balance for the production sector gives

$$\frac{d}{dt}M_p[Cl]_p = REC[Cl]_{rec} + RET[Cl]_{ret} - P[Cl]_p \qquad (2)$$

where M_p is the mass of fluid (in kg) in the production sector, REC is the recharge flow to production, RET is the flow injection fluid back to production and P is the flow of produced fluid. The model does not consider mass input of shallow boiled cool water.

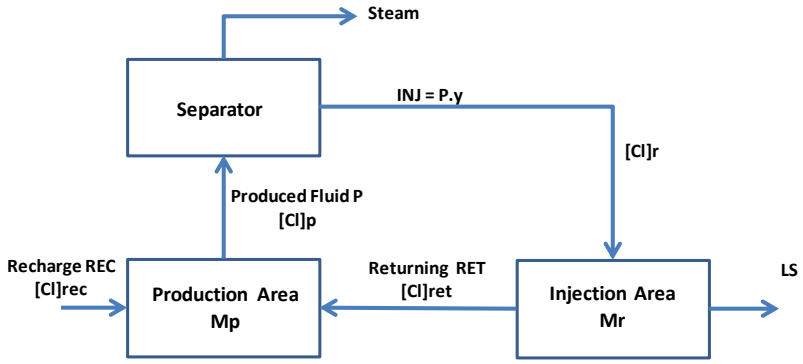

Figure 7: Production-injection lumped parameter model.

The symbols $[Cl]_p$, $[Cl]_{rec}$ and $[Cl]_{ret}$ refer to the chloride concentration of the production (total discharge), recharge and returning fluid respectively. The first assumption means that M_p is approximately constant and a total mass balance for the production sector gives:

$$REC + RET - P = 0$$

Then equation (2) reduces to

$$\frac{d}{dt}[Cl]_p = \frac{P}{M_p}\{(1-F)[Cl]_{rec} + F[Cl]_{ret} - [Cl]_p\} \quad (3)$$

where $F = \frac{RET}{P}$ and is the fraction of the injection fluid in the produced fluid. Similarly, a chloride mass balance for the injection sector gives

$$\frac{d}{dt}M_r[Cl]_{ret} = y.P[Cl]_r - LS[Cl]_{ret} - RET[Cl]_{ret} \quad (4)$$

where y is the water fraction from the separator, M_r is the mass of fluid in the injection area, $[Cl]_r$ is the injection line chloride and LS is the flow of injection fluid leaving the injection sector and not returning to the production sector. Mass conservation requires that $y.P = RET + LS$ and $[Cl]_p = y[Cl]_r$.

Therefore, equation (4) becomes

$$\frac{d}{dt}[Cl]_{ret} = \frac{P}{M_r}\{[Cl]_p - y[Cl]_{ret}\} \quad (5)$$

3.1 Analytic Solution for a Constant Production Rate

The two unknowns in equations (3) and (5) are $X = [Cl]_p$ the production chloride concentration and $Z = [Cl]_{ret}$ the chloride concentration from the injection sector to the production sector. Malate et al. (2016) presented analytic solution for a constant production rate P, where equation (3) becomes

$$\frac{dX}{dt} = \frac{P}{M_p}[A' + FZ - X] \quad (6)$$

where $A' = (1-F)[Cl]_{rec}$ and equation (5) becomes

$$\frac{dZ}{dt} = \frac{P}{M_r}[X - yZ]\,. \quad (7)$$

These two coupled linear ordinary differential equations can easily be solved using standard techniques to obtain

$$X(t) = C_1 \exp(\varphi_1 t) + C_2 \exp(\varphi_2 t) + X_\infty \quad (8)$$

$$Z(t) = b_1 C_1 \exp(\varphi_1 t) + b_2 C_2 \exp(\varphi_2 t) + Z_\infty \quad (9)$$

where X_∞ and Z_∞ are the steady state solutions reached after a long time.

The coefficients b_1 and b_2 are given by $b_j = \frac{1}{F}\left[\frac{\varphi_j}{q} + 1\right]$, $j = 1,2$.

Here $q = \frac{P}{M_p}$ and φ_1 and φ_2 are the two roots of the quadratic equation

$$M_p M_r \varphi^2 + (M_p y + M_r) P\varphi + (y - F)P^2 = 0 \quad (10)$$

The constants C_1 and C_2 are evaluated by using the initial conditions $X(0) = X_0$ and $Z(0) = Z_0$. They are given by:

$$C_1 = \frac{1}{(\varphi_1 - \varphi_2)}[q(FZ_0 - X_0 + A') - \varphi_2(X_0 - X_\infty)] \quad (11)$$

$$C_2 = \frac{1}{(\varphi_2 - \varphi_1)}[q(FZ_0 - X_0 + A') - \varphi_1(X_0 - X_\infty)] \quad (12)$$

The steady state solution of equation (6) gives the long term production chloride concentration given by

$$X_\infty = \frac{(1-F)[Cl]_{rec}}{(1-f)} \quad (13)$$

Here $f = \frac{RET}{INJ}$ is the fraction of the injection fluid returning. Also since $INJ = y.P$ and $F = \frac{RET}{P}$ then

$$f = \frac{F}{y} \quad (14)$$

3.2 Variable Production Rate Analytic Model

Malate et al (2016) also presented the variable production rate model where the rate is approximated by a piecewise constant function and then the constant rate analytic solution derived previously can be used in each of the intervals (t_i, t_{i+1}) as shown in Figure 8 below:

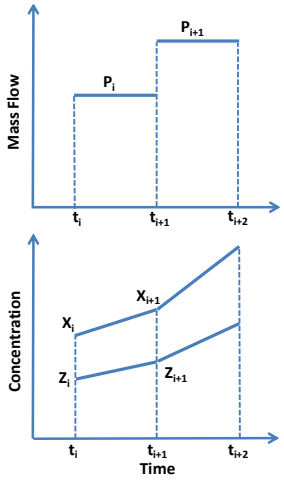

Figure 8: Step-function increase in mass flow and chloride concentration.

For t in the interval $t_i < t < t_{i+1}$ the solutions can be written as

$$X(t) = C_{1i} \exp \varphi_{1i}(t - t_i) + C_{2i} \exp \varphi_{2i}(t - t_i) + X_\infty \quad (15)$$

$$Z(t) = b_{1i} C_{1i} \varphi_{1i} \exp(t - t_i) + b_{2i} C_{2i} \exp \varphi_{2i}(t - t_i) + Z_\infty \quad (16)$$

Solving for the constants in equations (15) and (16) gives

$$C_{1i} = \frac{1}{(\varphi_{1i} - \varphi_{2i})}[G_i - \varphi_{2i}(X_i - X_\infty)] \quad (17)$$

$$C_{2i} = \frac{1}{(\varphi_{2i} - \varphi_{1i})}[G_i - \varphi_{1i}(X_i - X_\infty)] \quad (18)$$

where $G_i = q(FZ_i - X_i + A')$ and φ_{1i} and φ_{2i} are evaluated from the corresponding version of equation (10)

Therefore when $t = t_{i+1}$

$$X_{i+1} = C_{1i} exp \varphi_{1i} \Delta t_i + C_{2i} exp \varphi_{2i} \Delta t_i + X_\infty \quad (19)$$

where $\Delta t_i = t_{i+1} - t_i$ and

$$Z_{i+1} = b_{1i} C_{1i} exp \varphi_{1i} \Delta t_i + b_{2i} C_{2i} exp \varphi_{2i} \Delta t_i + Z_\infty \quad (20)$$

Then equations (17) to (20) provide a recurrence relationship between X_i , Z_i and X_{i+1}, Z_{i+1} which can be used to solve the problem beginning with known initial values for X_0 and Z_0.

3.3 Chloride Modelling Results

The analytic solutions for the two cases of firstly a constant and secondly a variable production rate derived above were used to match the observed changes in reservoir chloride concentration in SJ4-1 at the start of SJ10-1 brine injection (Jacobs 2015b). SJ4-1 recently presented a small decline in production enthalpy but was assumed to have remained essentially constant. A water fraction (y) of around 0.72 was then assumed which approximates the San Jacinto plant operating conditions. The model parameters used are listed in **Table 3**.

Table 3: Model data used to match SJ4-1 reservoir chloride.

Parameter	
Baseline reservoir chloride recharge $[Cl]_{rec}$	3200 - 3400 mg/kg
Initial production reservoir chloride $[Cl]_o$ in 2008	3450 mg/kg
Initial injection chloride returning $[Cl]_{ret}$	4800 mg/kg

The recharge chloride was assumed to be 2,800 mg/kg similar to the initial production chloride concentration at the start of exploitation in 2005. The initial production chloride used in the models, were taken during the start of brine injection in SJ10-1 at around 3,450 mg/kg. The initial injection chloride concentration returning was then evaluated from the amount of water separated at the wellhead and the initial production chloride concentration.

For the constant production rate model, an average mass flow of about 390 t/hr (~110 kg/s) was used. The parameters M_p and M_r have been lumped into a single parameter τ (i.e. $\tau = {M_p}/{M_r}$). As an initial approximation, it was also assumed that M_p is equal to M_r ($\tau = 1.0$). The tracer recoveries (~16%) obtained from the two reservoir tracer tests were then used as the initial fraction f of returning fluid to the production sector.

The two parameters M_p and fraction f were then adjusted to match the observed data given the initial model data from **Table 3**. After several trials, $M_p = 6.0E+09$ was found to give results approximating the observed trend of increasing chloride concentration. The fraction f was also slightly increased in an attempt to improve the match to the early data. The simulated results for the constant flow rate model with fraction $f = 0.20$ are shown in Figure 9. The model gave a fairly good fit to the observed data especially at early times. A poor match is however obtained at later times. It is noted that quite large variability in chloride concentration is observed during this time which could have been influenced by other factors such as enthalpy changes due to pressure drawdown or laboratory measurement and analysis. Laboratory data quality (ion balance) deteriorated in 2013 – 2014. Additionally, model results using fraction f higher than 0.20 produced a worse fit to reservoir chloride data.

The effect of changing τ (hence M_p) was also tested for a fraction f value of 0.20. The model results did not produce improved agreement against the observed data. Further experimentation showed that decreasing the value of τ improves the match at later times but not at early times.

The variable production rate model was also applied to match the production chloride concentration. An approximate production history of SJ4-1 was taken from spot TFT data from 2007-2014 in the absence of continuous regular production rate monitoring data that was only obtained after the installation of orifice plate flow metering device by the end of 2014. The results of the variable flow rate model are also presented in Figure 9 with $M_p = 6.0E+09$ kg and fraction $f = 0.20$. The variable analytic model produced a slightly improved fit to the observed data than the constant flow rate model. The best match also gave a fraction f consistent with the tracer recoveries obtained from reservoir tracer studies.

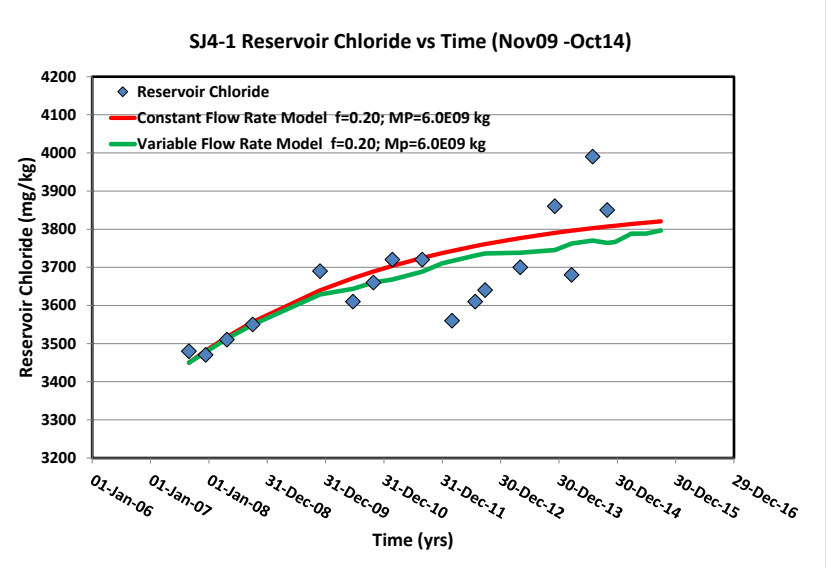

Figure 9: SJ4-1 production chloride and model results with time (2005-2014).

4. SIMPLE MODEL OF THERMAL DECLINE

The temperature decline observed in the production well is modelled by coupling the chloride mass balance to a one-dimensional fractured zone model following the work of Malate et al. (2016). An energy balance around the production block (see Figure 7) gives

$$V_p\left[(1-\phi)\rho_r c_r + \phi\rho_p c_p\right]\frac{d}{dt}T_p = -Pc_pT_p + RECc_{rec}T_{rec} + RETc_{ret}T_{ret}(t) \quad (21)$$

where T_p, T_{rec} and T_{ret} are the temperatures of the production, recharge and returning fluid respectively.

V_p is the total volume of the production sector
$\emptyset$ is the porosity
ρ_p density of production fluid
ρ_r and c_r density and heat capacity of rock matrix, in the production sector.

Also c_p, c_{rec} and c_{ret} are the heat capacities of the production, recharge and returning fluids respectively. These are assumed to be constant in the model. The recharge temperature T_{rec} is also assumed constant. The temperature of the returning fluid T_{ret} is a function of time determined by the mathematical model of the fractured zone containing the injection and production sectors.

The given initial conditions are

$$T_p(0) = T_0 \text{ and } T_{ret}(0) = T_0$$

where T_0 is the initial reservoir temperature. It is convenient to use T_0 as a base temperature and define

$$\theta_p = T_p - T_0 \qquad \text{and} \qquad \theta_{ret} = T_{ret} - T_0$$

Then equation (21) becomes

$$M_p(1+\varpi)\frac{d}{dt}\theta_p = -P\theta_p + RET\theta_{ret}(t) \quad (22)$$

and the transformed initial condition is $\theta_p(0) = 0$

Here the relationships $M_p = V_p\phi\rho_p$ and $P = REC + RET$ have been used and

$$\varpi = \frac{(1-\phi)\rho_r c_r}{\phi\rho_p c_p} \quad (23)$$

Rearranging the terms and simplifying gives

$$\frac{d}{dt}\theta_p + \xi\theta_P = \psi\theta_{ret}(t) \quad (24)$$

where $\xi = \frac{P}{[M_p(1+\varpi)]}$ and $\psi = \frac{RET}{[M_p(1+\varpi)]} = F\xi = fy\xi$

4.1 Fracture Zone Model

Since permeability in San Jacinto is generally controlled by structures, the main path for the return of injection fluids to the production area is provided by faults. A range of temperature models of the fractured zone can be considered where majority of the analytic models derived employs the heat transport by advection in the fracture with some heat diffusion into the impermeable rock matrix. The simple model described here envisages the zone as a highly fractured region containing many flow paths which allow the water to be in good contact with the fractured rock.

Single fracture model can also be considered that which allows for lateral diffusion of heat into the surrounding rock. The single fracture models all predict a first arrival of some thermal effects with the first arrival of injection water. The observed time lag where the chemicals/tracers arrive in about 28 days and thermal effects taking at least 400 days from the start of SJ10-1 injection in April 2008 can only be explained by a fractured zone which acts like a porous medium.

Then for one-dimensional flow, the equation for conservation of energy in the fracture zone is

$$\left[\left(1-\phi_f\right)\rho_r c_r + \phi_f\rho_l c_l\right]\frac{\partial T_f}{\partial t} + \rho_l c_l V\frac{\partial T_f}{\partial x} = K\frac{\partial^2 T_f}{\partial x^2} \quad (25)$$

where T_f is the temperature in the fractured zone, V is the Darcy velocity, ϕ_f is the porosity of the fractured zone and K is the thermal conductivity of the rock matrix. Both ρ_l the density and c_l the specific heat of the fluid moving in the fracture are assumed to be approximately independent of temperature.

Assuming the effect of heat conduction is negligible, equation (25) can also be written in terms of $\theta_f = T_f - T_0$ as a simple heat advection model

$$\frac{\partial\theta_f}{\partial t} + U\frac{\partial\theta_f}{\partial x} = 0 \quad (26)$$

Then the transformed initial and boundary conditions are

$\theta_f(x,0) = 0$ and $\theta_f(0,t) = \theta_1 = T_1 - T_0$ where T_1 is the injection temperature.

Here U is the thermal front velocity given by

$$U = \frac{V\phi_f\rho_l c_l}{[(1-\phi_f)\rho_r c_r + \phi_f\rho_l c_l]} \quad (27)$$

The thermal front is the transition zone where the temperature changes from the initial reservoir temperature T_0 to the injection temperature T_1.

Then in equation (24) becomes $\theta_{ret}(t) = \theta_f(L,t)$

where L is the distance between the production and injection areas.

The solutions for the production and returning fluid temperatures (equations (24) and (26)) can be derived using Laplace transforms.

The solution is

$$T_p = T_0 \quad \text{for } t \le t_T \quad (28)$$

$$T_p = T_0 + W\{1 - exp[-\xi(t - t_T)]\} \quad \text{for } t \ge t_T \quad (29)$$

where $W = \frac{\psi}{\xi}(T_1 - T_0)$

The symbol t_T is the time taken for the thermal front to travel the distance L and is defined by $t_T = {}^{L}/_{U}$.

4.1 Thermal Decline Modelling Results

From Figure 2, it can be seen that a fairly defined thermal decline in SJ4-1 occurred after about 400 days of injection into SJ10-1. The distance between production well SJ4-1 and injection well SJ10-1 is approximately 1.62 km. Hence the thermal front velocity can be easily evaluated as 4.05 m/day. Since the chemical (chloride) front has been observed to have occurred after about one month of production, the effective porosity ϕ_f for the fractured zone can be determined using

$$\frac{U}{V} = \frac{\phi_f\rho_l c_l}{[(1-\phi_f)\rho_r c_r + \phi_f\rho_l c_l]} \quad (30)$$

Assuming $\rho_r = 2{,}700$ kg/m^3, $c_r = 1.0$ kJ/kg-°K, $\rho_l = 790$ kg/m^3, and $c_l = 4.9$ kJ/kg-°K then from equation (32), the effective porosity is found to be approximately 5.0%.

The parameters used in matching the temperature decline in SJ4-1 are listed in **Table 4** below. An initial M_p of $6.0E+09$ kg and fraction of returning fluid $f = 0.20$ were used based on chloride modelling results. A constant injection temperature of 160°C is assumed in the model. The initial reservoir temperature used in the model was taken during the start of brine injection in SJ10-1 at around 258°C.

Table 4: Model data used to match SJ4-1 thermal decline.

Parameter	
Thermal front velocity U	4.05 m/day
Fraction of returning fluid f	0.38
Reservoir temperature T_0	258°C
Injection temperature T_1	160°C
Production rate P	390 t/hr (~110 kg/s)
Factor ϖ	0.50

Using the solution (equations 28 and 29) derived for the production temperature, the parameter ϖ was then varied to match the temperature decline. The model results for $\varpi = 1.05$ and fraction $f = 0.20$ are presented in Figure 10 below. The temperature model did not give a good match to the observed temperature decline. The model produced a slower temperature decline compared to the measured temperature data.

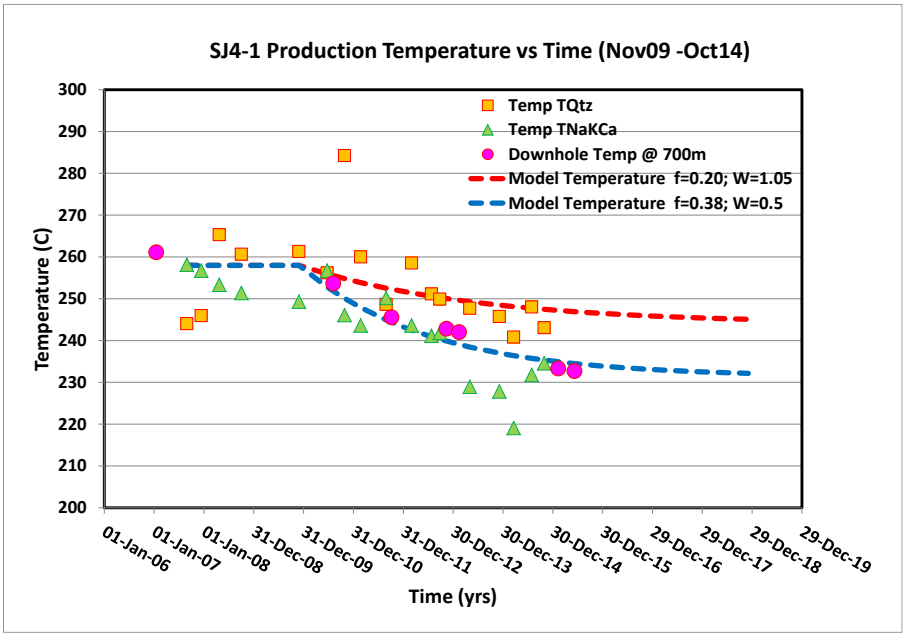

Figure 10: SJ4-1 temperature and model results with time (2009-2014).

It can be argued that additional input of cooler fluids may have caused the lower temperatures measured in the well. But there is no direct evidence of cooler groundwater incursion since the other geochemical parameters (i.e. SO_4, HCO_3, Mg) have been stable. Ingress of relatively cooler shallow boiled reservoir water may have then occurred in the well as suggested by the trends of chloride and $\delta^{18}O$ and $\delta^{2}H$ stable isotope data collected before SJ10-1 injection started in 2008. To date, there was a steady increase in chloride and $\delta^{18}O$ since 2005, with reasonably constant $\delta^{2}H$. The entry of this shallow boiled cool water may have been triggered by the pressure drawdown observed in the well.

The fraction of returning fluid f was then increased to match the temperature data, with the model results also shown in Figure 10. The temperature model with higher fraction $f = 0.38$ and $\varpi = 0.50$ produced a fairly good fit to the measure data. The thermal decline at SJ4-1 is then modelled to approach stable production temperature of around 230°C assuming continued constant production rate at 390 t/hr.

The effective porosity of the production block can then be calculated using equation 23. This was found to be around 5.8%, slightly higher than fracture porosity previously obtained.

The simple heat advection model gave a good approximation to the measured data with the assumption of negligible heat transport by conduction. The significance of lateral heat conduction can be investigated by allowing some heat diffusion from the fractured zone into the adjacent matrix. The fracture flow model that was derived did not improve the good match obtained using the simple heat advection model. Very small values of heat lost to the country rock were found from the match using the more complex fracture flow model. The small conductive heat effect could be attributed to the preferential permeability in a single direction observed in San Jacinto. This would mean there is high permeability along the major axis of mapped faults and lesser permeability perpendicular to it.

5. RESERVOIR MANAGEMENT STRATEGY

The results of reservoir tracer tests helped PENSA to understand possible connection of southern injection wells to the main production area together with the possible impact of limited injection closer to the production wells. This has informed changes to the location of injection and is an on-going process to balance pressure support with risks of reservoir cooling.

The favorable results of additional injection well SJ11-2, in the northern part of the field also provided PENSA the option to transfer the bulk of injection from the south (SJ1-1 and SJ10-1). Another reservoir tracer testing campaign for the northern injection wells (SJ11-1 and SJ11-2) and in-field injection well (SJ9-2 ST3) is underway to establish possible communication to the production wells. Initial results showed some level of communication between SJ12-1 ST1 and the nearby production wells. The results of these tracer tests will further provide PENSA the flexibility to optimize injection and sustaining the performance of the San Jacinto reservoir.

6. SUMMARY

The San Jacinto-Tizate Geothermal Production Field in Nicaragua was developed by Polaris Energy Nicaragua S.A. (PENSA) for power production since 2005. PENSA implemented reservoir management strategies for the sustainability of the resource through intensive monitoring, one of which is reservoir tracer testing.

A series of reservoir tracer tests using naphthalene disulfonate salts (NDS) was conducted by PENSA with the main objective of quantifying the rate and extent of brine injection returns from the northern, infield and southern injection wells to the central production wells. The tracer tests were conducted after commissioning of the condensing plants in 2011 and completing the production drilling and well remedial operations in January 2014.

Positive tracer returns were observed in production wells SJ4-1, SJ6-2 and SJ9-1 from the injection fluids coming from SJ10-1. The tracer return curves were processed and interpreted using simple radial flow tracer model. Modelling of NDS tracer recoveries in the affected wells gave a fraction of returning fluid ranging from 10% to 16%. The return of injection fluids into SJ4-1 has resulted in gradual decline in measured temperature in the well. This thermal decline is modelled by coupling the chloride mass balance model to a fracture flow model. The simple heat advection model satisfactorily represented the thermal decline observed in the well.

The reservoir tracer tests implemented in San Jacinto geothermal production field helped understand the hydrological connection of northern and southern injection wells to the main production area together with the impact of limited infield injection. The results of reservoir tracer testing have also provided PENSA the flexibility to optimize injection and balance pressure support against the risk of reservoir cooling.

REFERENCES

Anduril 2.3: Software for interpretation of tracer experiments for inter-well tests. Noldor S.R.L., Argentina, (2005).

Fossum, M.P. and Horne, R.N.: Interpretation of Tracer Return Profiles at Wairakei Geothermal Field Using Fracture Analysis, GRC Transactions, Vol 6, 261-264, (1982).

Jacobs: 2015 San Jacinto Reservoir Tracer Test, Report for PENSA, Auckland, New Zealand (2015a).

Jacobs: SJ4-1 Production Chloride and Temperature Lumped Parameter Modelling, Report for PENSA, New Zealand (2015b).

LaGeo: Septimo Informe de Inyeccion de trazadore químicos de sales sódicas de acidos naftalen sulfónicos en el campo geotermico de San Jacinto Tizate, Gerencia de Estudios y Evaluation. Santa Tecla, 31 de Agosto de 2015, (2015).

Malate, R.C.M. and O'Sullivan, M.J.: Modelling of Chemical and Thermal Changes in Well PN-26, Palinpinon, Philippines, *Proceedings,* 15th Workshop on Geothermal Reservoir Engineering, Stanford University, Stanford, CA, USA, (1990).

Malate, R.C.M., Prado, L.L and Guidos, J.A.: Modelling of Chemical and Thermal Changes in SJ4-1, San Jacinto-Tizate Geothermal Field, Nicaragua, *Proceedings,* 40th Workshop on Geothermal Reservoir Engineering, Stanford University, Stanford, CA, USA, (2016).

Rose, P., Johnson, S.D., and Kilbourn, P.: Tracer Testing at Dixie Valley Nevada, Using 2 Naphthalene Sulfonate and 2,7 Naphthalene Di-sulfonate; *Proceedings,* 26th Workshop on Geothermal Reservoir Engineering, Stanford University, Stanford, CA, USA, (2001).